Thymoquinone-induced autophagy mitigates doxorubicin-induced H9c2 cell apoptosis

DAWEI LIU[1] and LEI ZHAO[2]

Departments of [1]Cardiovascular Surgery and [2]Nephropathy, Xijing Hospital,
The Fourth Military Medical University, Xi'an, Shanxi 710032, P.R. China

Abstract. Doxorubicin (Dox)-induced myocardiopathy is a massive obstacle in administering chemotherapeutic drugs in cancer patients. In the present study, the effects of thymoquinone (TQ) on Dox-induced cardiotoxicity were investigated *in vitro*. H9c2 cardiomyocytes were pre-treated with TQ followed by Dox, and cell viability and cell death were subsequently measured. Flow cytometry was conducted to evaluate the apoptosis of H9c2 cells. Autophagy was assessed by immunofluorescence LC3 staining. Western blot analysis was performed to determine autophagy-, apoptosis- and LKB1/AMPK-related proteins. Dox-induced H9c2 cell death and apoptosis were decreased after pretreatment with TQ *in vitro*. The number of autophagosomes and autophagic markers was further increased by TQ in the Dox-treated H9c2 cells, which mediated LKB1/AMPK activation and the deactivation of mTOR. Suppression of autophagosomes abolished the TQ-induced antiapoptotic effect. In conclusion, TQ reduces Dox-induced apoptosis of cardiomyocytes by upregulating autophagy through activation of the LKB1/AMPK pathways. These novel results highlight the therapeutic potential of TQ to prevent Dox cardiotoxicity.

Introduction

Chemotherapy is the primary approach in the clinic for cancer treatment (1). Doxorubicin (Dox) is a quinone-containing anthracycline antibiotic widely used in clinics, frequently used for the treatment of multiple types of cancer, including breast cancer, lung cancer, sarcomas, as well as leukemia. It is one component in the CHOP regimen for lymphoma. However, the consequent dose-limiting cardiotoxicity is a significant obstacle to the application of Dox and a chief limiting factor in delivering optimal chemotherapy to cancer patients (2). Hence, investigating novel approaches to prevent Dox-induced cardiotoxicity is urgently needed.

It has been identified that several molecular pathogenesis processes are involved in Dox-induced cardiotoxicity (3), including accumulation of reactive oxygen species (ROS), mitochondrial damage, mitochondrial iron accumulation, transcription alterations, as well as DNA damage repair (4). Moreover, it has been widely illustrated that autophagy reduction in cardiomyocytes may be responsible for the cardiotoxicity of Dox (5). Hence, autophagy acts as a potential target for preventing Dox-induced cardiotoxicity.

Thymoquinone (2-isopropyl-5-methylbenzo-1, 4-quinone) (TQ), the most abundant constituent of the volatile oil also present in the fixed oil, is the biologically active compound of *Nigella sativa* seeds (6). Several studies have suggested the capacity of TQ on immunomodulatory and anti-inflammatory effects (7). Earlier researh demonstrated that TQ showed significant protective effects against Dox-induced cardiotoxicity in rats (8). More recently, a series of studies suggested that the inhibition of oxidative stress levels may be responsible for TQ action on the protective effects of cardiotoxicity (9,10). However, the potential mechanism of TQ on the protection of Dox-induced cardiotoxicity is still not fully understood. In the present study, novel mechanisms of action involved in the TQ-induced protective effects of cardiotoxicity were found to be related to an increased autophagy level and decreased apoptosis. Further mechanistic study suggested that TQ significantly increased AMP-activated protein kinase (AMPK) pathway activity. Our study may provide novel approaches to avoid cardiotoxicity when administering Dox in cancer patients.

Materials and methods

Cell culture. The H9c2 (rat heart-derived embryonic myoblast) cell line was purchased from the American Type Culture Collection (ATCC). The H9c2 cells were passaged 10 to 25 times before conducting experiments. Cells were cultured in Dulbecco's modified Eagle's medium (DMEM; Gibco; Thermo Fisher Scientific, Inc.), referred to as a high-glucose medium, supplemented with 10% fetal bovine serum (FBS) and 100 U/ml of penicillin/streptomycin within cultured dishes incubated at 37˚C in a humidified atmosphere

Correspondence to: Dr Lei Zhao, Department of Nephropathy, Xijing Hospital, The Fourth Military Medical University, 127 Changlexi Road, Xi'an, Shanxi 710032, P.R. China
E-mail: zhaolei314100@163.com

of 5% CO_2. After application of 0.5% FBS-supplemented DMEM for 24 h, H9c2 cardiomyocytes were subjected to treatment with Dox (Energy Chemical) for 24 h or pretreatment with TQ (Energy Chemical) for 30 min before Dox. To analyze the consequence of whether autophagy exerts apoptosis, cells were pretreated with bafilomycin A1 (Energy Chemical) for 30 min before exposure to TQ or Dox for 24 h.

CCK-8 and lactate dehydrogenase (LDH) assays for H9c2 cells. The CCK-8 (Sigma-Adrich; Merck KGaA) and LDH (Promega Corp.) assays were conducted to evaluate H9c2 cell proliferation. The H9c2 cells were harvested and plated into 96-well plates at a final concentration of $5x10^5$ cells per well. The cells were pretreated with TQ (5 and 10 μM) 30 min before administration of Dox (5 μM). After another 24-h incubation at 37°C, CCK-8 solution (10 μl) was added to each well. After incubation for 4 h, the optical density (OD) values were detected at 450 nm. For the LDH detection assay, LDH reagent was added to the collected culture medium incubated for 30 min at room temperature (RT), protected from light. Then, the OD value was quantified by a spectrophotometer at 490 nm. The cell survival rates (%) of the different groups were determined by dividing the OD value of the experimental group by the control group in the CCK-8 assays. The relative cell death rate (%) was calculated by dividing the OD value of the experimental group by the control group in the LDH assays.

Apoptosis detection in the H9c2 cells. The apoptosis of H9c2 cells was conducted using an Annexin V-FITC Apoptosis Detection Kit (Solarbio) according to the manufacturer's instructions. Cells were fixed with cold 70% ethanol for 1 h and then centrifuged and washed twice using cold PBS. Then the cells were incubated with Annexin V (1X) and propidium iodide (PI) (1X) for 30 min in the dark. The cells were washed twice again with PBS and re-suspended with detection buffer. An Accuri C6 flow cytometer (BD Biosciences) was used to detect apoptotic cells. The quantification was analyzed by Flowjo 7.6.5 software (Becton-Dickinson and Company).

Immunofluorescence. The H9c2 cells were fixed with 4% paraformaldehyde for 15 min at RT. Subsequently, the cells were washed with NaCl/Pi, permeabilized with 0.2% Triton X-100, and then were incubated with the LC3B primary rabbit antibody (cat: 3868; 1:100) at 4°C overnight. Cells were then incubated with Alexa 594-conjugated goat-anti-rabbit secondary antibody (cat: 8889, 1:200) for 1 h at 37°C. The images were captured by DMi8 fluorescence microscope (x400 magnification) (Leica Microsystems GmbH). The LC3 puncta were measured by ImageJ software (v1.8.0) (National Institutes of Health, Bethesda, MD, USA).

Western blot analysis. Homogenates of H9c2 cells were used for western blot analysis. Protein (30 μg per lane) was separated on a 10% gel by SDS-PAGE and transferred to a PVDF membrane. The membranes were blocked with 5% skim milk in 1X Tris-buffer containing 0.1% Tween-20 for 1 h. The blots were incubated overnight with primary antibodies, including apoptosis, autophagic protein markers, and key molecules in the AMPK pathway. Rabbit-cleaved caspase-3 (cat: 9664), LC3B (cat: 3868), phosphorylated (p-)LKB1 (cat: 3050), LKB1 (cat: 3055), AMPKα (cat: 5832), p-AMPKα (Thr172) (cat: 50081), p-ULK1 (Ser555) (cat: 5869), p-ULK1 (Ser317) (cat: 37762), ULK1 (cat: 8054), mTor (cat: 2972), p-mTOR (cat: 5536), and β-actin (cat: 3700) (dilution 1:1,000, Cell Signaling Technology, Inc.), were incubated with the membranes at 4°C overnight, which were further incubated with anti-rabbit horseradish peroxidase (HRP)-conjugated secondary antibody (cat: 7074) (dilution 1:2,000; Cell Signaling Technology, Inc.) for 1 h at RT. The blots were developed with an ECL chemiluminescence detection reagent (Bio-Rad Laboratories, Inc.). The protein bands were visualized by a ChemiDoc XRS+ Imager (Bio-Rad Laboratories, Inc.). ImageJ software (v1.8.0) was used to analyze the relative intensity.

Statistics. The data were analyzed by GraphPad 8.00 software (GraphPad Software, Inc.). The data are expressed as the mean $\pm$ SD, of three independent experiments. Unpaired Student's t-test was used to carry out the significance comparing 2 groups. Multigroup comparisons of the means were carried out by one-way analysis of variance (ANOVA) test with post hoc contrasts by Student-Newman-Keuls test when comparing groups $\leq$3. For groups >3, Tukey's test was conducted as a post hoc test. Student's t-test was used for two group comparisons. Statistical significance for all tests was set at $P<0.05$ (*).

Results

TQ reverses Dox-induced H9c2 cell death. Firstly, to choose the non-toxic concentration of TQ, the CCK-8 assay was conducted. As shown in Fig. 1A, no significant toxicity of TQ on H9c2 cells was noted under 10 μM after a 24-h incubation. Subsequently, as described in 'Materials and methods' section, cells were pre-treated with TQ and Dox was administrated for subsequent CCK-8 assay of cell viability. As illustrated in Fig. 1B, administration of Dox (5 μM) significantly decreased the viability of H9c2 cells, while TQ significantly reversed the inhibition of Dox-induced H9c2 cell viability. LDH assay was further conducted to evaluate cell death after co-administrated of Dox and TQ. As shown in Fig. 1C, although Dox significantly induced H9c2 cell death, TQ significantly decreased the cell death of H9ce cells in a dose-dependent manner. As shown in Fig. 1B and 1C, dexrazoxane (DEX) was used as a positive control, which is the only clinically approved drug for anthracycline-induced myocardial damage. These results preliminarily demonstrated that TQ is a candidate cardio-protective molecule, for which its mechanisms should be studied further.

TQ antagonizes Dox-induced apoptosis of H9c2 cells. Flow cytometry was conducted to evaluate the effects of the co-administration of Dox and TQ on H9c2 cell apoptosis. As shown in Fig. 2A, Dox (5 μM) significantly induced H9c2 cell apoptosis. The apoptotic cells under Dox treatment were approximately 20%. Pre-treatment with TQ significantly and dose-dependently decreased the Dox-induced apoptosis. These results further verified that TQ can recover H9c2 cell proliferation under Dox treatment.
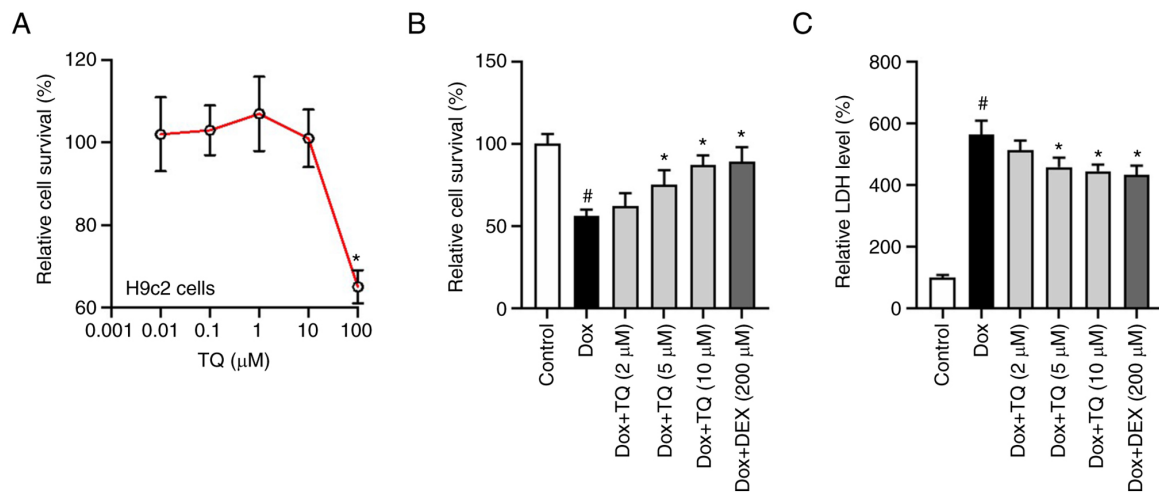
Figure 1. Effects of TQ pre-administration with Dox treatment on cardiomyocyte cell viability. (A) H9c2 cells were incubated with different concentrations of TQ for 24 h. The CCK-8 cell viability assay was performed according to the manufacturer's protocols. Cytotoxicity was not observed when the dose of TQ was <10 μM. (B) H9c2 cardiac myocytes were pre-treated with the indicated concentration of TQ for 30 min followed by Dox treatment. After 24 h, CCK-8 cell viability assay was performed. The cell viability was calculated by the dividing experimental group OD values by the control group OD values. (C) H9c2 cardiac myocytes were pre-treated with the indicated concentration of TQ for 30 min followed by Dox treatment. After 24 h, LDH cell death assay was performed. Data are presented as the mean ± SD of three independent experiments. A one-way ANOVA test with post hoc Tukey's test was used for evaluating the difference. Significance was indicated at P<0.05: #P<0.05, vs. the control group; *P<0.05, vs. the Dox group. LDH, lactate dehydrogenase; TQ, thymoquinone; Dox, doxorubicin; OD, optical density.
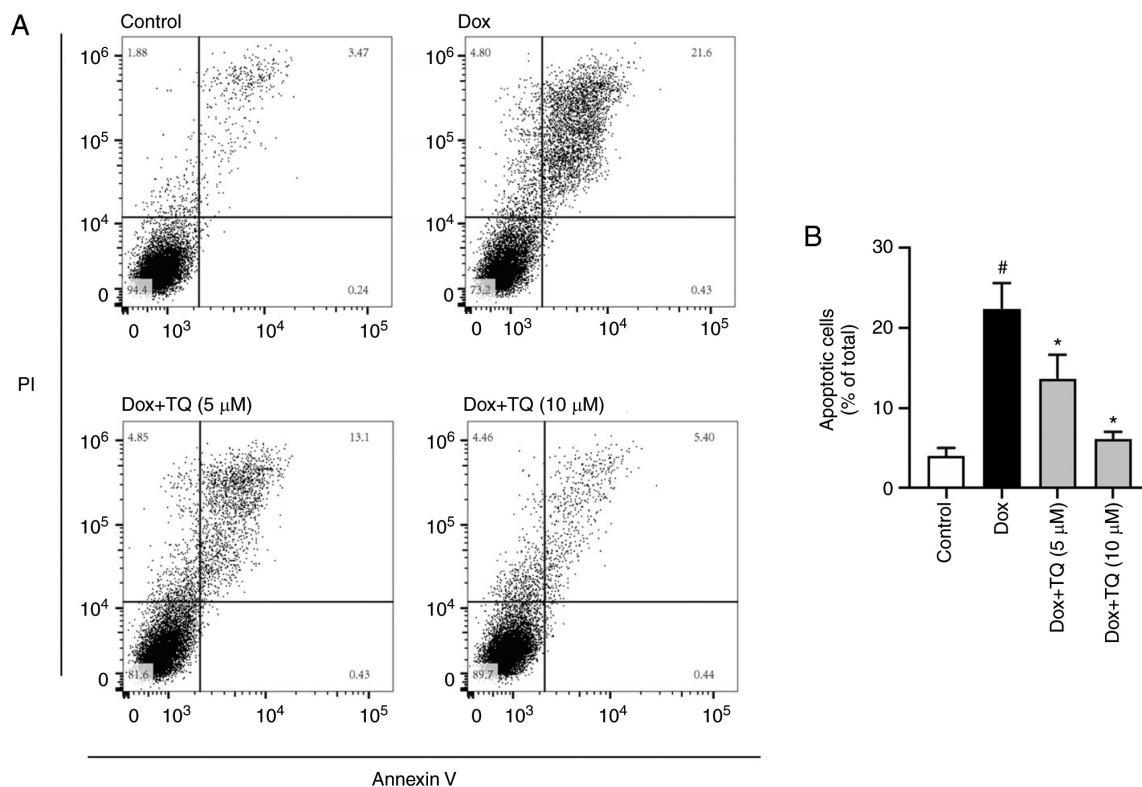

Figure 2. Effects of TQ pre-administration with Dox treatment on cardiomyocyte apoptosis. (A) The Annexin V/PI double staining flow cytometry analysis is shown as dot plots after treatment with Dox and/or TQ. The x-axis indicates the Annexin V-positive cell population, while the y-axis illustrates the PI-positive cell population. (B) The quantitative results of A were determined by calculating the percentages of the Annexin V-positive and Annexin V/PI-double positive cell populations. Data are presented as the mean ± SD of three independent experiments. A one-way ANOVA test with post hoc Tukey's test was used for evaluating the differences. Significance was indicated at P<0.05: #P<0.05 vs. the control group; *P<0.05, vs. the Dox group. TQ, thymoquinone; Dox, doxorubicin.

TQ regulates autophagy in H9c2 cells. Autophagy protein LC3 was visualized by immunofluorescence. As shown in Fig. 3A and B, the percentage of LC3 puncta formation in Dox-treatment H9c2 cells was upregulated. However, in the TQ co-treatment groups, the rate of LC3 puncta formation was significantly and potently increased in a dose-dependent
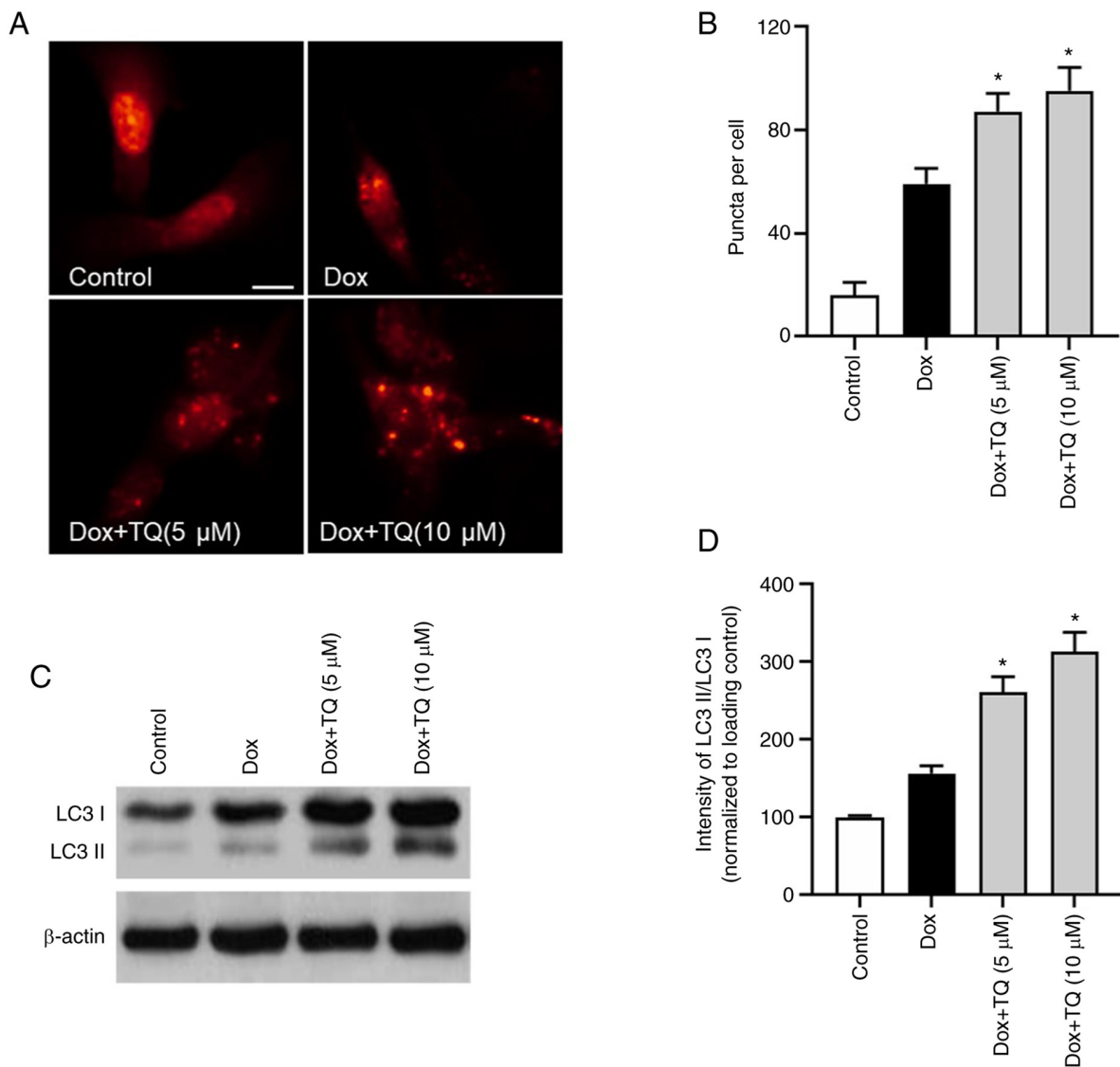
Figure 3. Doxorubicin-induced autophagic cell numbers increase with TQ pre-treatment. (A) Representative LC3 staining were observed in H9c2 cells incubated with Dox with or without TQ (5 and 10 μM) pretreatment to evaluate formation of autophagosomes (scale bar, 100 μm). (B) Statistical analysis of the number of LC3 puncta per cell in A as evaluated by Image J software. (C) Representative blot of autophagic markers in H9c2 cells after co-administration of TQ and Dox. (D) The intensity of the LC3II/LC3I ratio normalized to the loading control. Data are presented as the mean ± SD of three independent experiments. A one-way ANOVA test with post hoc Tukey's test was used for evaluating the differences. Significance was indicated at P<0.05: *P<0.05, vs. the Dox group. TQ, thymoquinone; Dox, doxorubicin; LC3, microtubule-associated protein 1A/1B-light chain 3.

manner, which indicated that TQ treatment upregulated the autophagy level in the H9c2 cells. Furthermore, as shown in Fig. 3C and D, western blot analysis of LC3 protein showed that, after co-treatment with TQ, the LC3II/LC3I ratio was significantly upregulated, suggesting that TQ regulated autophagy in the H9c2 cells.

TQ-induced autophagy regulates Dox-induced apoptosis in H9c2 cells. To assess the role of TQ-induced autophagy in Dox-mediated apoptosis, H9c2 cells were pretreated with bafilomycin A1, an inhibitor of autophagic flux by disruption of vacuolar-type H$^+$-ATPase. Bafilomycin (Baf) pretreatment restored the decreased percentage of apoptotic cells (Fig. 4A and C). In addition, the TQ-induced increase in the ratio of LC3II to LC3I was enhanced with bafilomycin (Fig. 4B and D). Moreover, bafilomycin pretreatment also increased active caspase-3 expression (Fig. 4B and E). These

results indicated that the activation of autophagy may be responsible for reversing apoptosis in H9c2 cells induced by TQ.

TQ decreases Dox-mediated H9c2 cell cytotoxicity by activating the LKB1/AMPK/ULK1 axis. Western blot analysis was conducted to evaluate the effect of TQ on AMPK-related molecules. As shown in Fig. 5A-C, the expression levels of phosphorylated (p-)LKB1, p-AMPKα, and p-ULK1 at Ser317 were significantly increased after TQ treatment, indicating that activation of LKB1/AMPK signaling is responsible for the mechanisms of action of TQ. Moreover, the expression levels of p-mTOR and p-ULK1 at Ser575 were significantly decreased after TQ treatment, which further verified that the activation of AMPK signaling is a crucial mechanism of TQ-mediated reversal of the apoptosis induced by Dox in H9c2 cells.
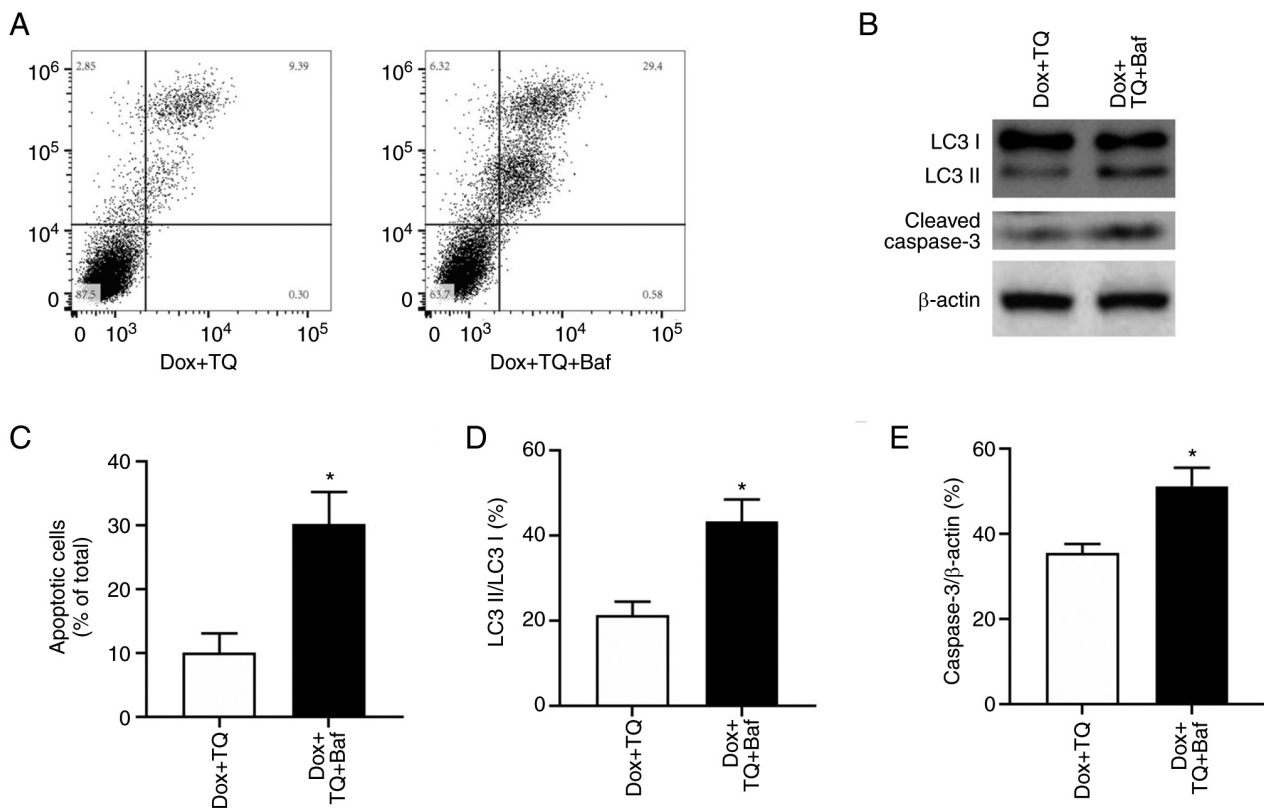
Figure 4. Anti-apoptotic effect of TQ is mediated by autophagy. Cells were pre-treated with Baf (1 nM) for 30 min prior to exposure to TQ (5 μM) and Dox for 24 h. (A) The Annexin V/PI double staining flow cytometry analysis is shown as dot plots after treatment with Dox and TQ, and pre-treatment with Baf. (B) Autophagic and apoptosis markers in H9c2 cells were determined by western blot assay after treatment with Dox and TQ, and pre-treatment with Baf. (C) Representative apoptotic cells of H9c2 in A. (D) The percentage of LC3II/LC3I in B. (E) Representative intensity of cleaved-caspase-3 in B. Data are presented as the mean ± SD of three independent experiments. Student's t-test was used for evaluating the difference. Significance was indicated at P<0.05: *P<0.05, vs. the Dox+TQ group. Baf, bafilomycin A1; TQ, thymoquinone; Dox, doxorubicin.

Discussion

Chemotherapeutic drug-induced cardiomyopathy is a complication associated with high morbidity during chemotherapy (11). Doxorubicin (Dox) is an anthracycline drugs which has been utilized for anti-neoplastic therapy for several years. Nevertheless, cardiac toxicity induced by Dox greatly limits its further application, and is always difficult to predict, remaining the most prevalent side effect threatening the survival of patients (12,13). Although adequate treatment strategies may decrease the risk of cardiotoxicity of Dox, the prognosis of Dox-induced heart failure remains uncertain or uncontrollable (14). Hence, the investigation of novel strategies for preventing myocardial cells from Dox-induced toxicity is still urgently needed.

Thymoquinone (TQ) is one of the most abundant constituents of the volatile oil (also present in the fixed oil) and is a biologically active compound of *Nigella sativa* seeds. TQ has been documented as exhibiting a series of bioactivities on anti-inflammatory, antioxidant, anti-cancer, as well as antimicrobial properties (15-18). Previously, TQ has shown promising roles against oxidative damage-induced free radical agents and Dox, which induce cardiotoxicity. It exerts suppressive activity on carcinogenesis, eicosanoid production, and membrane lipid peroxidation. Moreover, TQ works as an effective chemo-protective phytochemical, and destroys Fe-NTA-induced oxidative stress (19-21). In

the present study, we reported the novel protective effects of TQ on Dox-induced cardiotoxicity in an H9c2 cell *in vitro* model. TQ showed significant protective effects against Dox-induced H9c2 cell death. This result was in accordance with recent documented studies (9,22). Based on this finding, we further evaluated the potential mechanisms of action of the TQ effects on protecting Dox-induced cardiotoxicity. The apoptotic rates in H9c2 cells were significantly decreased by TQ administration, indicating the definite protective effects of TQ on Dox-induced cardiotoxicity. Dox-induced cardiotoxicity is involved in a series of molecular mechanisms and signaling pathways, including oxidative stress, autophagy, iron metabolism, and inflammation (23). More recently, it has been indicated that dysregulation of autophagy plays a vital role in Dox-induced cardiotoxicity (24), and a series of natural products were reported to activate the protective effects on cardiotoxicity by inducing autophagy (25-27). Hence, the potential autophagy influenced by TQ was evaluated in H9c2 cells after Dox treatment. As expected, the autophagy level was significantly upregulated after administration of TQ. Therefore, we hypothesized that the mechanisms of action of TQ were involved in inducing protective autophagy in Dox-treated H9c2 cells and preventing apoptosis, thereby preventing cardiotoxicity.

The autophagy inhibitor bafilomycin A1 was used to verify the results. After co-treatment with bafilomycin A1, the TQ-induced myocardial cell protection effect was diminished.
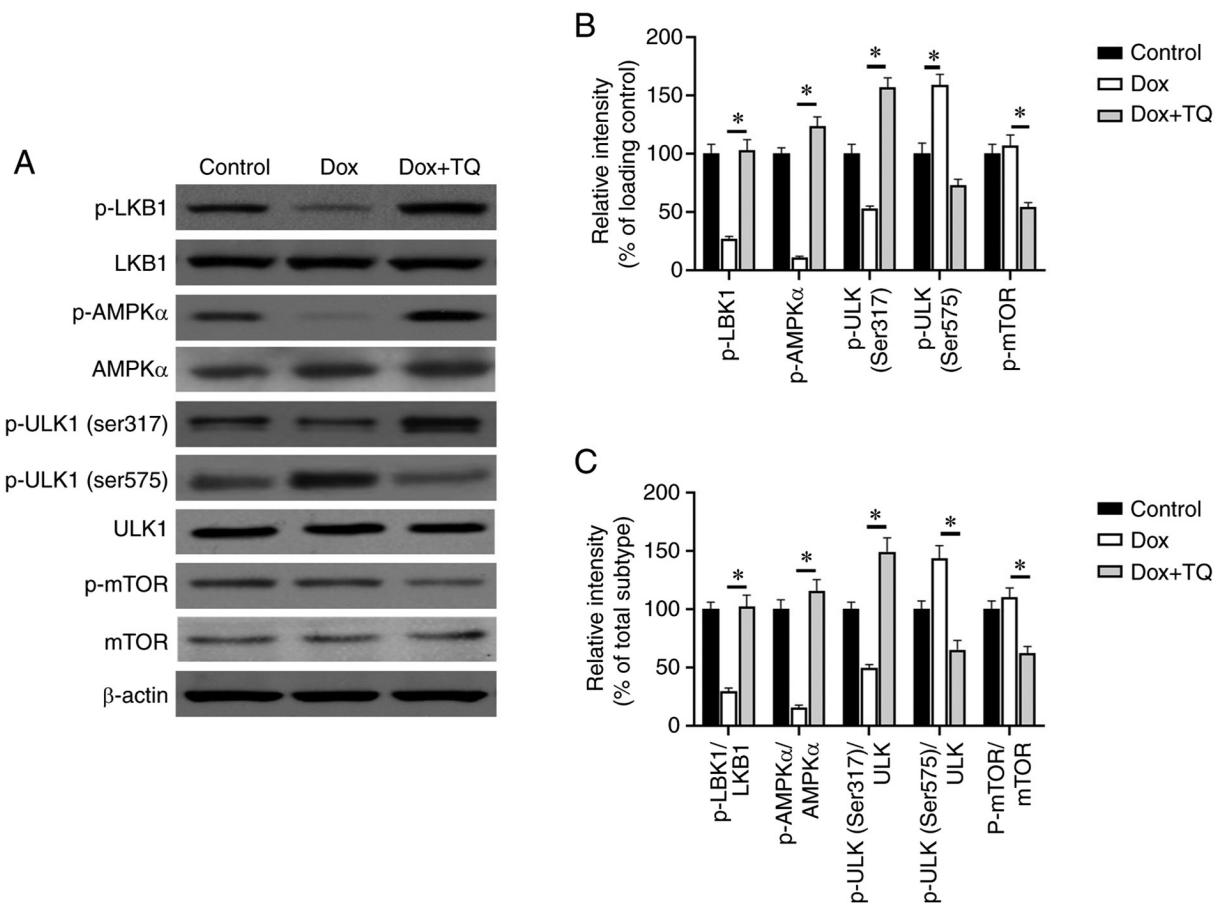
Figure 5. TQ activates the LKB1/AMPK/ULK1 pathway. (A) Western blot analysis shows the expression of p-LKB1, LKB1, p-AMPKα, AMPKα, p-ULK1 (ser317), p-mTOR, and p-ULK1 (ser575) after Dox or Dox in combination use with TQ. (B) Relative intensity (% of loading control) of p-LKB1, LKB1, p-AMPKα, AMPKα, p-ULK1 (ser317), p-mTOR, and p-ULK1 (ser575) after Dox or Dox in combination use with TQ which was determined by Image J software. (C) Relative intensity (% of total subtype) of p-LKB1, LKB1, p-AMPKα, AMPKα, p-ULK1 (ser317), p-mTOR, and p-ULK1 (ser575) after Dox or Dox in combination use with TQ which was determined by Image J software. Data are presented as the mean ± SD of three independent experiments. A one-way ANOVA test with post hoc Student-Newman-Keuls test was used for evaluating the difference. Significance was indicated at P<0.05: *P<0.05, Dox vs. the Dox+TQ group. TQ, thymoquinone; Dox, doxorubicin; LKB1, liver kinase B1; AMPK, AMP-activated protein kinase; ULK1, unc-51-like kinase 1; mTOR, mammalian target of rapamycin; p-, phosphorylated.

Moreover, western blot assays showed that after bafilomycin A1 co-administration, autophagy- and apoptosis-related proteins came back to the level of the Dox-treated group only. These findings demonstrated that TQ prevents Dox-induced H9c2 cell apoptosis through induction of autophagy.

Autophagy is able to be mediated by several pathways. For example, the kinase mTOR is a critical regulator of autophagy induction, with activated mTOR (Akt and MAPK signaling) suppressing autophagy and negative regulation of mTOR (AMPK and p53 signaling) promoting it (28). In the present study, after screening a series of signaling pathways, we found that the activation of LKB1/AMPK and downregulation of mTOR activity were involved in the mechanisms of action of TQ. In the aforementioned western blot assays, TQ was able to significantly upregulate the level of phosphorylated (p-)LKB1 and p-AMPK in the TQ+Dox group, compared with that in the Dox group. Moreover, the level of p-mTOR and its downstream molecule, p-ULK1 (ser575) was downregulated in the TQ+Dox group. In addition, the expression level of neither AMPK nor mTOR were significantly altered. These results indicated that the activation of the LKB1/AMPK pathway is responsible for the protective effects of TQ in the H9c2 cell model.

Candidate drugs for treating degenerative diseases are responsible for producing toxicity (29). Although in our evaluation, TQ showed less toxicity in H9c2 cells, it is necessary to understand the potential toxic effects and safety and risk for possible human use. One of the positive characteristics of bioactive compounds of medicinal plants is their low toxicity, which demonstrates promising and prominent effects in health management (30,31). For TQ, it is documented that no toxic effects were found toward fibroblast-like synoviocytes at less than 10 μM. In addition, TQ supplementation did not show any toxic effect on the liver and reduced the aspartate aminotransferase (AST) and alanine aminotransferase (ALT) levels in treated rats (32). Moreover, two studies indicated that an acceptable dose of TQ (0.6 mg/kg/day) is suitable for humans (33,34). The above information preliminarily confirms that TQ is a safe bioactive agent for humans.

TQ has also been subjected to intensive exploration in regards to its toxicity, appropriate dose, and upper tolerable limit through various animal-based efficacy trials. The outcomes of most of the trials confirmed that TQ does not display any toxic effect within the range of 10-100 mg/kg

body both in subchronic and subacute doses (35). Moreover, Gali-Muhtasib *et al* (36) found that TQ exhibited its anti-oncogenic perspective at minimum doses of 5-20 mg/kg rather than its reported LD_{50} value. Several investigations revealed no side effect of TQ prolonged consumption at 10-100 mg/kg for up to 20 weeks (36). Hence, these sufficient shreds of evidence indicate that TQ is a safe agent for humans, and well-designed clinical trials in humans are required to confirm these effects for Dox-induced cardiotoxicity patients.

While this study was being conducted, it was documented that TQ could attenuate Dox-induced cardiotoxicity in rats, which further verify our positive results (9). In addition, our study further indicated the potential and novel mechanisms of action of TQ on protective effects of cardiomyocytes, which has not yet been reported. Hence, based on multiple evidence, TQ is a potential active molecule and provides insight for further evaluation on antagonizing anthracycline-induced cardiotoxicity.

In conclusion, TQ has been preliminarily confirmed to be a potential candidate for protecting Dox-induced cardiotoxicity. The mechanisms of action involved in the TQ-mediated cardioprotective effects consist in the upregulation of autophagy in cardiomyocytes. However, well-designed clinical trials in humans are required to confirm these effects for Dox-induced cardiotoxicity in these patients.

Availability of data and materials

The datasets used and/or analyzed during the current study are available from the corresponding author on reasonable request.

Authors' contributions

DL and LZ were involved in conducting the experiments, and collecting and analyzing the data. DL and LZ confirm the authenticity of all the raw data. DL contributed to the research methodology and writing of the original draft. LZ was responsible for writing, review of the manuscript and editing. All authors read and approved the final manuscript and agree to be accountable for all aspects of the research in ensuring that the accuracy or integrity of any part of the work are appropriately investigated and resolved.

Ethics approval and consent to participate

Not applicable.

Patient consent for publication

Not applicable.

Competing interests

The authors declare that they have no competing interests.

References

1. Gotwals P, Cameron S, Cipolletta D, Cremasco V, Crystal A, Hewes B, Mueller B, Quaratino S, Sabatos-Peyton C, Petruzzelli L, *et al*: Prospects for combining targeted and conventional cancer therapy with immunotherapy. Nat Rev Cancer 17: 286-301, 2017.
2. Tan TC, Neilan TG, Francis S, Plana JC and Scherrer-Crosbie M: Anthracycline-induced cardiomyopathy in adults. Compr Physiol 5: 1517-1540, 2015.
3. Octavia Y, Tocchetti CG, Gabrielson KL, Janssens S, Crijns HJ and Moens AL: Doxorubicin-induced cardiomyopathy: From molecular mechanisms to therapeutic strategies. J Mol Cell Cardiol 52: 1213-1225, 2012.
4. Zhang S, Liu X, Bawa-Khalfe T, Lu LS, Lyu YL, Liu LF and Yeh ET: Identification of the molecular basis of doxorubicin-induced cardiotoxicity. Nat Med 18: 1639-1642, 2012.
5. Li DL, Wang ZV, Ding G, Tan W, Luo X, Criollo A, Xie M, Jiang N, May H, Kyrychenko V, *et al*: Doxorubicin blocks cardiomyocyte autophagic flux by inhibiting lysosome acidification. Circulation 133: 1668-1687, 2016.
6. Ali BH and Blunden G: Pharmacological and toxicological properties of *Nigella sativa*. Phytother Res 17: 299-305, 2003.
7. Shaterzadeh-Yazdi H, Noorbakhsh MF, Hayati F, Samarghandian S and Farkhondeh T: Immunomodulatory and anti-inflammatory effects of thymoquinone. Cardiovasc Hematol Disord Drug Targets 18: 52-60, 2018.
8. Nagi MN and Mansour MA: Protective effect of thymoquinone against doxorubicin-induced cardiotoxicity in rats: A possible mechanism of protection. Pharmacol Res 41: 283-289, 2000.
9. Karabulut D, Ozturk E, Kaymak E, Akin AT and Yakan B: Thymoquinone attenuates doxorubicin-cardiotoxicity in rats. J Biochem Mol Toxicol 35: e22618, 2021.
10. Pehlivan DY, Durdagi G, Oyar EO, Akyol S and Ozbek M: The effects of melatonin and thymoquinone on doxorubicin-induced cardiotoxicity in rats. Bratisl Lek Listy 121: 753-759, 2020.
11. Curigliano G, Cardinale D, Suter T, Plataniotis G, de Azambuja E, Sandri MT, Criscitiello C, Goldhirsch A, Cipolla C, Roila F and ESMO Guidelines Working Group: Cardiovascular toxicity induced by chemotherapy, targeted agents and radiotherapy: ESMO clinical practice guidelines. Ann Oncol 23 (Suppl 7): vii155-166, 2012.
12. Robertson ID, Naprasnik A and Morrow D: The sources of pesticide contamination in Queensland livestock. Aust Vet J 67: 152-153, 1990.
13. Wenningmann N, Knapp M, Ande A, Vaidya TR and Ait-Oudhia S: Insights into doxorubicin-induced cardiotoxicity: Molecular mechanisms, preventive strategies, and early monitoring. Mol Pharmacol 96: 219-232, 2019.
14. Al-Malky HS, Al Harthi SE and Osman AM: Major obstacles to doxorubicin therapy: Cardiotoxicity and drug resistance. J Oncol Pharm Pract 26: 434-444, 2020.
15. Ali MY, Akter Z, Mei Z, Zheng M, Tania M and Khan MA: Thymoquinone in autoimmune diseases: Therapeutic potential and molecular mechanisms. Biomed Pharmacother 134: 111157, 2021.
16. Gholamnezhad Z, Havakhah S and Boskabady MH: Preclinical and clinical effects of *Nigella sativa* and its constituent, thymoquinone: A review. J Ethnopharmacol 190: 372-386, 2016.
17. Imran M, Rauf A, Khan IA, Shahbaz M, Qaisrani TB, Fatmawati S, Abu-Izneid T, Imran A, Rahman KU and Gondal TA: Thymoquinone: A novel strategy to combat cancer: A review. Biomed Pharmacother 106: 390-402, 2018.
18. Isaev NK, Chetverikov NS, Stelmashook EV, Genrikhs EE, Khaspekov LG and Illarioshkin SN: Thymoquinone as a potential neuroprotector in acute and chronic forms of cerebral pathology. Biochemistry (Mosc) 85: 167-176, 2020.
19. Abdel-Daim MM, Abo El-Ela FI, Alshahrani FK, Bin-Jumah M, Al-Zharani M, Almutairi B, Alyousif MS, Bungau S, Aleya L and Alkahtani S: Protective effects of thymoquinone against acrylamide-induced liver, kidney and brain oxidative damage in rats. Environ Sci Pollut Res Int 27: 37709-37717, 2020.

20. Nili-Ahmadabadi A, Alibolandi P, Ranjbar A, Mousavi L, Nili-Ahmadabadi H, Larki-Harchegani A, Ahmadimoghaddam D and Omidifar N: Thymoquinone attenuates hepatotoxicity and oxidative damage caused by diazinon: An in vivo study. Res Pharm Sci 13: 500-508, 2018.
21. Alam MF, Khan G, Safhi MM, Alshahrani S, Siddiqui R, Sivagurunathan Moni S and Anwer T. Thymoquinone ameliorates doxorubicin-induced cardiotoxicity in swiss albino mice by modulating oxidative damage and cellular inflammation. Cardiol Res Pract 2018: 1483041, 2018.
22. Öztürk E, Kaymak E, Akin A, Karabulut D, Ünsal HM and Yakan B: Thymoquinone is a protective agent that reduces the negative effects of doxorubicin in rat testis. Hum Exp Toxicol 39: 1364-1373, 2020.
23. Timm KN and Tyler DJ: The role of AMPK activation for cardioprotection in doxorubicin-induced cardiotoxicity. Cardiovasc Drugs Ther 34: 255-269, 2020.
24. Dirks-Naylor AJ: The role of autophagy in doxorubicin-induced cardiotoxicity. Life Sci 93: 913-916, 2013.
25. Shabalala S, Muller CJF, Louw J and Johnson R: Polyphenols, autophagy and doxorubicin-induced cardiotoxicity. Life Sci 180: 160-170, 2017.
26. Ma Y, Yang L, Ma J, Lu L, Wang X, Ren J and Yang J: Rutin attenuates doxorubicin-induced cardiotoxicity via regulating autophagy and apoptosis. Biochim Biophys Acta Mol Basis Dis 1863: 1904-1911, 2017.
27. Xu ZM, Li CB, Liu QL, Li P and Yang H: Ginsenoside Rg1 prevents doxorubicin-induced cardiotoxicity through the inhibition of autophagy and endoplasmic reticulum stress in mice. Int J Mol Sci 19: 3658, 2018.
28. Codogno P, Mehrpour M and Proikas-Cezanne T: Canonical and non-canonical autophagy: Variations on a common theme of self-eating? Nat Rev Mol Cell Biol 13: 7-12, 2011.
29. Khan N and Sultana S: Inhibition of two stage renal carcinogenesis, oxidative damage and hyperproliferative response by Nigella sativa. Eur J Cancer Prev 14: 159-168, 2005.
30. Vance SH, Benghuzzi H, Wilson-Simpson F and Tucci M: Thymoquinone supplementation and its effect on kidney tubule epithelial cells in vitro. Biomed Sci Instrum 44: 477-482, 2008.
31. Mu GG, Zhang LL, Li HY, Liao Y and Yu HG: Thymoquinone pretreatment overcomes the insensitivity and potentiates the antitumor effect of gemcitabine through abrogation of notch1, PI3K/Akt/mTOR regulated signaling pathways in pancreatic cancer. Dig Dis Sci 60: 1067-1080, 2015.
32. Qadri SM, Mahmud H, Föller M and Lang F: Thymoquinone-induced suicidal erythrocyte death. Food Chem Toxicol 47: 1545-1549, 2009.
33. Khader M, Bresgen N and Eckl P: In vitro toxicological properties of thymoquinone. Food Chem Toxicol 47: 129-133, 2009.
34. Dollah MA, Parhizkar S, Latiff LA and Bin Hassan MH: Toxicity effect of Nigella sativa on the liver function of rats. Adv Pharm Bull 3: 97-102, 2013.
35. Abukhader M: The effect of route of administration in thymoquinone toxicity in male and female rats. Indian J Pharm Sci 74: 195, 2012.
36. Gali-Muhtasib H, Kuester D, Mawrin C, Bajbouj K, Diestel A, Ocker M, Habold C, Foltzer-Jourdainne C, Schoenfeld P, Peters B, et al: Thymoquinone triggers inactivation of the stress response pathway sensor CHEK1 and contributes to apoptosis in colorectal cancer cells. Cancer Res 68: 5609-5618, 2008.